



ISSN: 0067-2904  
GIF: 0.851

## Computer Generation of Low Light-Level Images

Raaid N. Hassan\*, Huda S. Ali

Department of Astronomy and space, College of Science, University of Baghdad-Iraq.

### Abstract:

As result of exposure in low light-level are images with only a small number of photons. Only the pixels in which arrive the photopulse have an intensity value different from zero. This paper presents an easy and fast procedure for simulating low light-level images by taking a standard well illuminated image as a reference. The images so obtained are composed by a few illuminated pixels on a dark background. When the number of illuminated pixels is less than 0.01% of the total pixels number it is difficult to identify the original object.

**Keywords:** Poisson distribution, low light-level image, Astronomical Imaging, Photon-Limited Images.

### توليد حاسوبي لصور ذات مستوى ضوئي واطئ

رائد نوفي حسان\*، هدى شاكر علي

قسم الفلك والفضاء، كلية العلوم، جامعة بغداد-العراق

### الخلاصة:

النتيجة لالتقاط صور بمستوى ضوئي واطئ هي صور ذات عدد قليل من الفوتونات. النقاط التي تصل اليها نبضه فوتونيه (ضوئية) هي فقط التي تمتلك شدة تختلف عن الصفر. قدم هذا البحث طريقة سهلة وسريعة لمحاكاة الصور ذات المستوى الضوئي الواطئ وذلك باخذ صورة ذات اضاءته معيارية جيدة كمرجع والصور المحصلة مكونة من نقاط مضيئة في خلفية سوداء. عندما كان عدد النقاط المضيئة اقل من 0.01% من العدد الكلي كان من الصعوبة تحديد الجسم الاصل.

### Introduction

Low light-level images arise in many applications such as night vision, laser radar, radiological imaging, high energy astronomical imaging, and others. Has described experiment on the absolute sensitivity of the human visual system [1-4]. The spatial coordinates of detected photoevents and the number of detected photoevents in a given area convey information about the classical high light-level irradiance of the scene. The fundamental question that we address is: "How many detected photons are needed in the input scene to distinguish or identify a reference object from a set of background (or noise) images?" In the present work the reference image is used as the system impulse response. In an actual recognition system one can encounter changes in scale and orientation of the image as well.

### Astronomical Imaging

Weak celestial bodies of steady and constant luminance emit very few photons and hence are relatively difficult to detect. The two main imaging devices that are used in astronomical imaging for such observations are photomultipliers and charge-coupled devices (CCD), which can be briefly specified as follows:

\*Email: raadnoffi742000@yahoo.com

- Photoelectric devices called photomultiplier tubes were commonly used in the early 1950's in the field of astronomy for the measurement of starlight. Photons that strike the surface of such device respond by emitting an electron according to the photoelectric effect. The electron is then accelerated by an electrical field, and then hits another surface called a dynode which generates three electrons. The process is repeated until a pulse of electrons is generated, hence leading to a pulse-counting procedure in a given time interval. Since the measurement depends on the number of photons counted, it follows a Poisson distribution. [5,6].

- Charge-coupled device (CCD) is an array of microscopic square-shaped light-sensitive cells, referred to as photosites, which converts photons to electricity linearly, i.e. the more photons strike a photosite, the more charge is produced by it, thereby leading to an increased brightness at the corresponding pixel. The linearity property of CCD arrays has made them widely used in astronomical imaging [4], covering a wide range of frequencies, nearly all ultra-violet to X-ray applications. As the pixel values generated by a CCD array are proportional to the number of photons that reach its photosites, the grey-levels of resulting images have to follow a Poisson process [7-9].

Both the aforementioned methods can also suffer from additional degradation introduced by blurring artifacts. In particular, before reaching the imaging device, the electromagnetic waves have to penetrate the Earth atmosphere. Differences in the temperature distribution and the speed of wind across different layers of the atmosphere result in a random distribution of its diffraction index which, in turn, results in a linear blurring effect [9]. Therefore, deblurring procedures can potentially improve the quality of such measurements.

**The Poisson Distribution**

The Poisson distribution is a discrete probability law which determines the probability with which a positive integer is observed, given a positive real parameter which is equal to both the mean and variance of the distribution. In practice, the Poisson probability law can be interpreted as defining a probability measure for a counting process of events (sometimes called arrivals), which took place at a specified time interval [10-11]. In this interpretation, the parameter of the distribution is equal to the product of the temporal duration of the interval and a specific arrival rate. The distribution, which was originally formalized by Simon-Denis Poisson (1781–1840), is given by [9]:

$$P_r(k) = \frac{e^{-\gamma T} (\gamma T)^k}{k!} \quad k \geq 0$$

Where  $e$  is the base of the natural logarithm ( $e = 2.71828\dots$ ),  $\gamma$  (*events/time*) is the arrival rate of the events,  $T$  [*time*] is the time interval of the counting process and  $k$  is the number of occurrences of the event.

**Photon-Limited Images**

At low levels of illumination, an input scene can be described in a binomial form. The detected image is composed of a set of photo-pulses distributed over a dark background, and hence, can be represented as a collection of Dirac-delta functions [12][13][14]:

$$\hat{I}(r, t) = \sum_{k=1}^N \delta(r - r_k(t)) \quad \dots \dots \dots (1)$$

where  $r_k$  represents the spatial coordinates of the  $k$ -th detected photo-pulse and  $N$  is the total number of detected photo-pulses. If the photo-pulses are collected by a detector of area  $A$  for a fixed time interval  $T$ , the conditional probability distribution for detecting  $N$  photo-pulses in the time interval  $[t, t+T]$  is an inhomogeneous Poisson process given by:

$$P(N) = \frac{1}{N!} \left[ \int_t^{t+T} dt' \int_A \gamma(r, t') dr \right]^N \exp \left[ - \int_t^{t+T} dt' \int_A \gamma(r, t') dr \right] \dots \dots \dots (2)$$

in which  $\gamma(r, t) = \mu I(r, t)/h\nu$  where  $\mu$  is the quantum efficiency of the detector,  $I(r,t)$  is the classical image irradiance,  $h$  is Planck's constant and  $\nu$  the incident light frequency.

In those cases in which  $I(r,t)$  does not fluctuate significantly, the ensemble average produces the following observable counting distribution[14-15]:

$$P(N) = \frac{\bar{N}^N}{N!} e^{-\bar{N}} \quad \dots \dots \dots (3)$$

where  $\bar{N} = \frac{\mu T}{h\nu} \int_A I(r) dr$ , It can also be seen that the probability density function for photo-pulse coordinates is given by [16,17-18]:

$$P(r) = \frac{I(r)}{\int_A I(r') dr'} \quad \dots \dots \dots (4)$$

### Simulation of Photon-Limited Images

The previous section described the statistical behavior of photon-limited or low light-level images. This will now be used in the simulation procedure, low light-level images of a given high light-level scene can be generated using a Poisson random number generator.

For a low light-level image the input Poisson parameter  $E_{ij}$  is chosen as follows:

- 1) Consider an image of area  $A$ , which has pixels of area  $\Delta A$ , and suppose that the average number of detected photoevents in the entire image is to be  $\bar{N}$ . From photo detection theory, the Poisson parameter for the  $ij$ th picture element is:

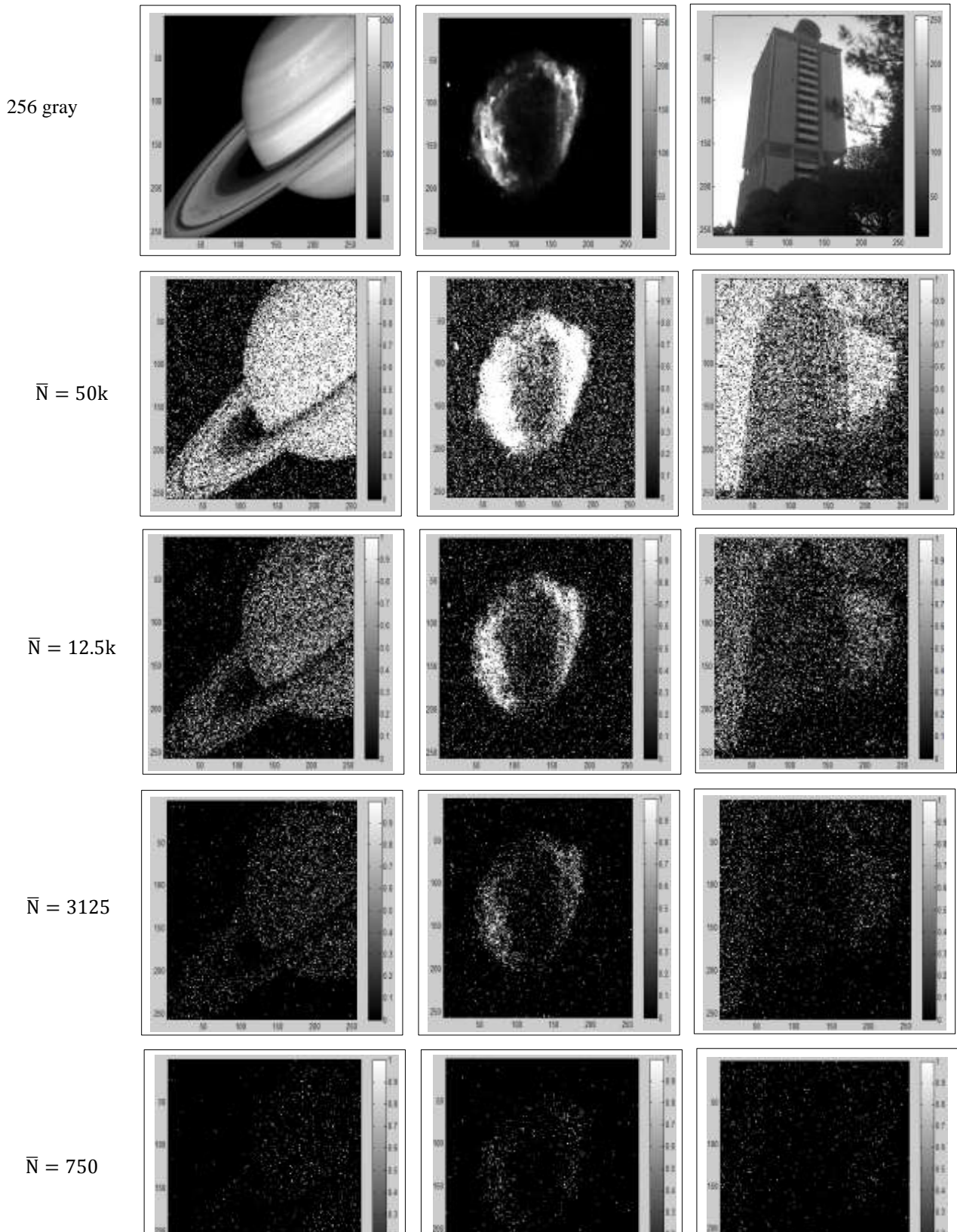
$$E_{ij} = \frac{\bar{N} I(x_i, y_j) \Delta A}{\iint_A dx' dy' I(x', y')} \quad \dots \dots \dots (5)$$

where  $I(x_i, y_j)$  is the high light-level irradiance of the pixel at spatial coordinates  $(x_i, y_j)$ , and  $\iint_A dx' dy' I(x', y')$  represent the total intensity of the input image.

- 2) A low light-level image can be produced from a corresponding high light-level scene by calling a Poisson random generator with parameter  $E_{ij}$  at each pixel in the associated high light-level image.
- 3) This simulation method allows us to obtain images with the same characteristics as those taken with a low light-level camera. Computer generation of low light-level images is shown in figure-1: first column, Saturn rings; second column, G1.9+0.3 galaxy; third column, The Baghdad university tower.

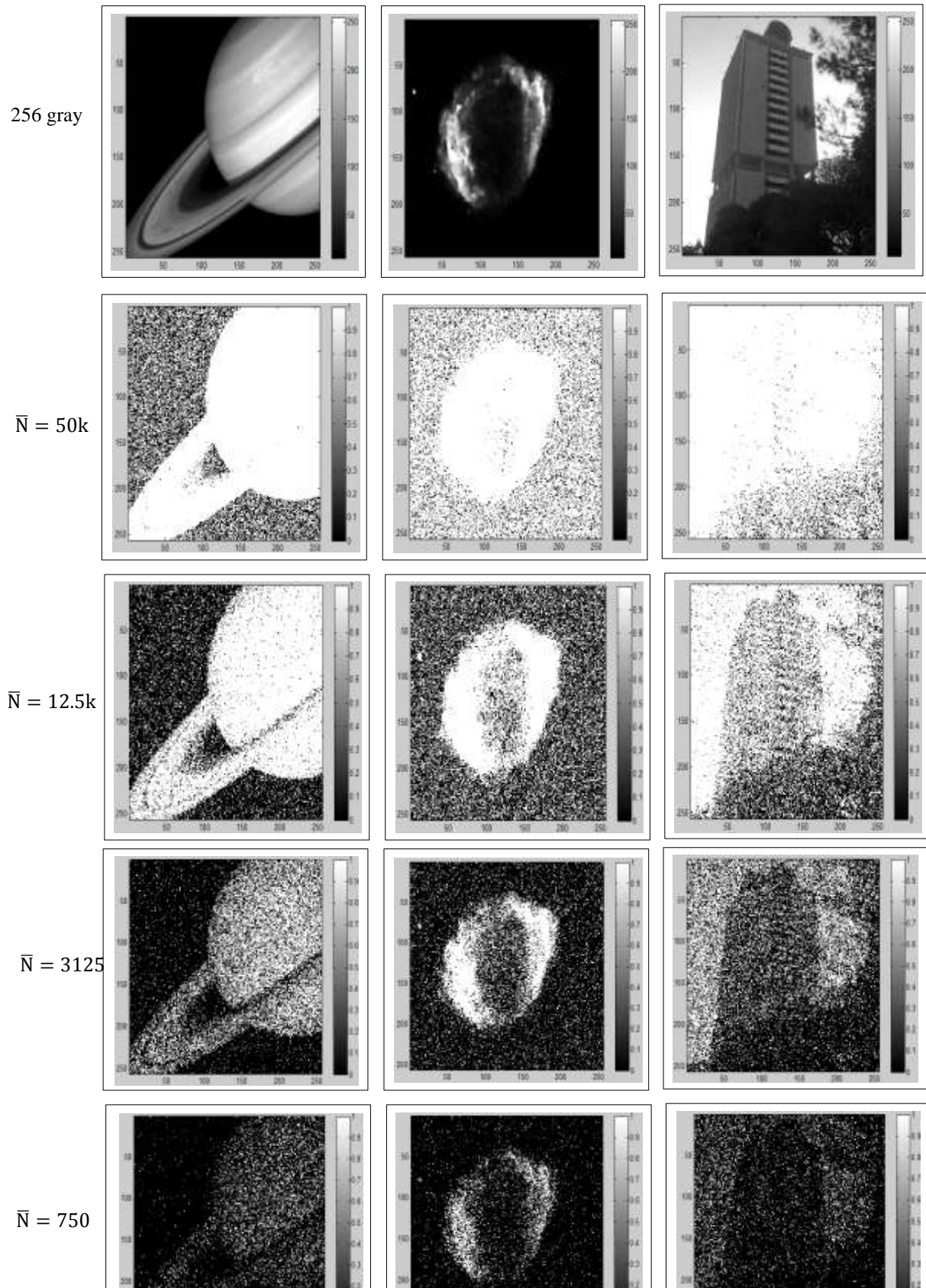
The high light-level images contain 256 gray levels.  $\bar{N}$  is the average number of detected photoevents over the entire image.

Figure-2 shows the effect of the size of the pixel area ( $\Delta A$ ) in the resulted simulation images, when the  $\Delta A$  is increases the bright image value will be increased. Analysis of a synthetic image and its resulting low level image further proved the output to be Poissonian images (The fact that the mean value of the low level image is almost equal to its variance), according to the table -1, this statistical property can be achieved only in the images have low number of photo-pulses or photoevents ( $N$ ) and small pixel area.



**Figure 1-** Computer-generated low light-level images: first column, Saturn rings; second column, G1.9+0.3 galaxy; third column, The Baghdad university tower. The high light-level images contain 256 gray levels.  $\bar{N}$  is the average number of detected photoevents over the entire image. With  $\Delta A=1$  pixel.





**Figure 2-** Computer-generated low light-level images: first column, Saturn rings; second column, G1.9+0.3 galaxy; third column, The Baghdad university tower. The high light-level images contain 256 gray levels.  $\bar{N}$  is the average number of detected photoevents over the entire image. With  $\Delta A=10$  pixel.

**Table 1-** statistical property for three low light-level images (Saturn rings, G1.9+0.3 galaxy; Baghdad university tower), each table contain different pixel area and different average number (N) of detected photoevents over the entire image with its mean and variance.

Saturn		Mean = 89.8678		Variance=6.68E+03		Galaxy		Mean = 23.0396		Variance=1.89E+03		
Pixel area ΔA=1		Pixel area ΔA=10		Pixel area ΔA=1		Pixel area ΔA=10		Pixel area ΔA=1		Pixel area ΔA=10		
N	mean	variance	mean	variance	N	mean	variance	mean	variance	N	mean	variance
50000	0.7574	1.2241	7.6238	55.5102	50000	0.7647	2.831	7.6066	213.1871	50000	0.7617	1.0518
12500	0.1913	0.2191	1.9078	4.9259	12500	0.1923	0.3204	1.9069	14.9449	12500	0.1907	0.2085
3125	0.0469	0.0485	0.4792	0.6739	3125	0.0479	0.0554	0.4744	1.2831	3125	0.0482	0.0488
750	0.0111	0.0112	0.1145	0.1248	750	0.0108	0.011	0.1147	0.1634	750	0.0118	0.0119

Baghdad university tower		Mean = 115.69		Variance=6.75E+03			
Pixel area ΔA=1		Pixel area ΔA=10		Pixel area ΔA=10			
N	mean	variance	mean	variance	N	mean	variance
50000	0.7617	1.0518	7.6419	36.9666	50000	0.7617	1.0518
12500	0.1907	0.2085	1.9054	3.7417	12500	0.1907	0.2085
3125	0.0482	0.0488	0.4723	0.5851	3125	0.0482	0.0488
750	0.0118	0.0119	0.1133	0.1192	750	0.0118	0.0119

**Conclusion**

Presented an approach for representing and processing the low light-level image analysis using simple and fast algorithm. When the number of photons and pixel area are small, the measurement process is best modeled with a Poisson distribution.

The fact that the mean value of the noise is equal to its variance implies that the higher the values of the original image, the more severe is their contamination by noise. This fact creates the major difficulty in restoration of Poissonian images.

When the number of illuminated pixels in the noisy low light-level image is less than the 0.8% of the total pixels number it's proved the output to be Poisson.

**References:**

1. El-gayar, M. M., Soliman, H., meky. N. **2013**. A Comparative Study of Image Low Level Feature Extraction Algorithms, *Egyptian Informatics Journal*, 14, pp: 175–181.
2. Rose, A. **1948**. The Sensitivity Performance of the Human Eye on an Absolute Scale, *J. Opt. Soc. Am.* 38 (2), pp. 196-208.
3. Rose, A. **1977**. *Vision Human and Electronic*, Plenum press, New York-London, pp: 13-14.
4. White, J. T., and Subhashis G. **2011**. Bayesian Smoothing of Photon-Limited Images with Applications in Astronomy, *Journal of the Royal Statistical Society: Series B (Statistical Methodology)*, 73 (4), pp: 579–599.
5. McLean, I. S. **1997**. *Electronic Imaging in Astronomy: Detectors and Instrumentation*, John Wiley and Sons, pp: 13-15.
6. Ientilucci, E. J. **2000**. Synthetic Simulation and Modeling of Image Intensified CCDs (IICCD), M.Sc. thesis, College of science, Rochester Institute of Technology, pp: 27-31.
7. Khan, M.A.U., Khan, T.M., Khan, R.B., Kiyani, A., and Khan, M.A. **2012**. Noise Characterization in Web Cameras using Independent Component Analysis, *INT J COMPUT COMMUN*, ISSN 1841-9836, 7(2), pp: 302-311.
8. Healey, G. E., and Kondepudy, R. **1994**. Radiometric CCD Camera Calibration and Noise Estimation, *IEEE Trans. Pattern Anal. Machine Intel.* 16(3), pp: 267–276.
9. Bradt, H. **2004**. *Astronomy Methods: A Physical Approach to Astronomical Observations*, Cambridge University Press, pp: 137-145.

10. Grinstead C. M., and Snell, J. L. **1997**. *Introduction to Probability*, AMS, 2<sup>nd</sup> Edition, pp: 197-198.
11. Shaked, E. **2009**. A Novel Approach to Restoration of Poissonian Images, M.Sc. Thesis, Department of Electrical and Computer Engineering, Applied Science, University of Waterloo, Waterloo, Ontario, Canada.
12. Krishnamurthy, K., Raginsky, M., Willett, R. **2010**. Multiscale Photon-Limited Spectral Image Reconstruction, *SIAM J. Imaging Sci.*, 3(3), pp: 619–645.
13. Willett, R. M., Nowak, R. D. **2003**. Platelets: A Multiscale Approach for Recovering Edges and Surfaces in Photon-Limited Medical Imaging, *IEEE Transactions on Medical Imaging*, 22(3), pp: 332-350.
14. Arsenault, H. H., Makuow, B., Szoplik, T. **1989**. *Optical Processing and Computing*, Academic Press, Elsevier Inc., London, pp: 347-349.
15. Cagigal, M. P., Prieto, P. **1991**. Recovery from Low Light Level Images, Education in Optics, Proc. Soc. Photo-Opt. Instrum. Eng. Proceedings of the SPIE Education in Optics'91, San Petersburg, Russia, pp: 496-503, 9-14 Jul.
16. Goodman, J. W. **1985**. *Statistical Optics*, Willey-Interscience, New York, pp: 52-53.
17. Willett, R., and Nowak, R. **2004**. Fast Multiresolution Photon-Limited Image Reconstruction, Biomedical Imaging: Nano to Macro, *IEEE International Symposium*, 2, pp: 1192-1195.
18. Morris, G. M. **1989**. Opto-Electronic Random Number Generating System and Computing System Based Thereon, *University of Rochester, N. Y.*, Appl, 664893.